

Chinese Journal of Nuclear Physics, Vol. 16, No. 2, 1994, pp. 100-107
Atomic Energy Press, Beijing—Printed in P. R. China

The Production of ^{11}C and ^{17}F Secondary Radioactive Beams*

Bai Xixiang, Liu Weiping, Qin Jiuchang, Li Zhichang, Zhou Shuhua, Zhou Junfeng,
Li Anli, Wang Youbao, Guan Xialing and Wang Xiaozhong
(*China Institute of Atomic Energy, P. O. Box 275(46), Beijing 102413*)

Received 13 January 1994

Abstract— ^{11}C and ^{17}F secondary beams have been successfully tuned on the CIAE secondary radioactive beam line at the HI-13 tandem accelerator. The setting parameters of the secondary beam line and the beam quality for ^{11}C and ^{17}F are given. A ^{11}C beam is produced with intensity 1.2×10^5 particles / s and energy 41 ± 1.0 MeV.

Key words— ^{11}C , ^{17}F , Secondary beam, Secondary beam line.

1 INTRODUCTION

Up to now, most knowledge on nuclear physics has been obtained from nuclear reactions induced by ion beams of stable isotopes. The radioactive nuclear beams provide a new opportunity for studying nuclear phenomena in a wider degree of freedom of isospin. Since nuclear reactions which produce energy and synthesize new elements at various astrophysical sites in the cosmos often involve radioactive nuclei in their entrance channels, the nuclear data of the secondary radioactive beam induced reactions are of fundamental importance for verifying the theory of the evolution of the universe.

Recently, many laboratories have made great efforts in producing the secondary radioactive beams for nuclear physics research⁽¹⁾. The present paper describes the testing and tuning experiments of the ^{11}C and ^{17}F beams with China's first radioactive nuclear beam line (GIRAFFE), which has been built at the CIAE HI-13 tandem accelerator.

2 PRINCIPLE

The CIAE secondary beam line makes use of the inverted kinematics. The low energy heavy ions from the HI-13 tandem accelerator are used to bombard ^1H or ^2H targets to produce ^6He , ^7Be , ^8Li , ^{11}C , ^{12}B , ^{13}N , ^{15}O and ^{17}F radioactive nuclei. Because of the kinematic effect, these radioactive products are compressed into a forward cone. By using a dipole and a pair of quadrupoles, the desired radioactive isotope is separated from the primary beam and focused onto a secondary reaction target for studying the nuclear reactions of interest. The detailed discussion of the production reactions and the beam optics can be found in Refs. [2,3].

* The project supported in part by National Natural Science Foundation of China and China Nuclear Industry Science Foundation.

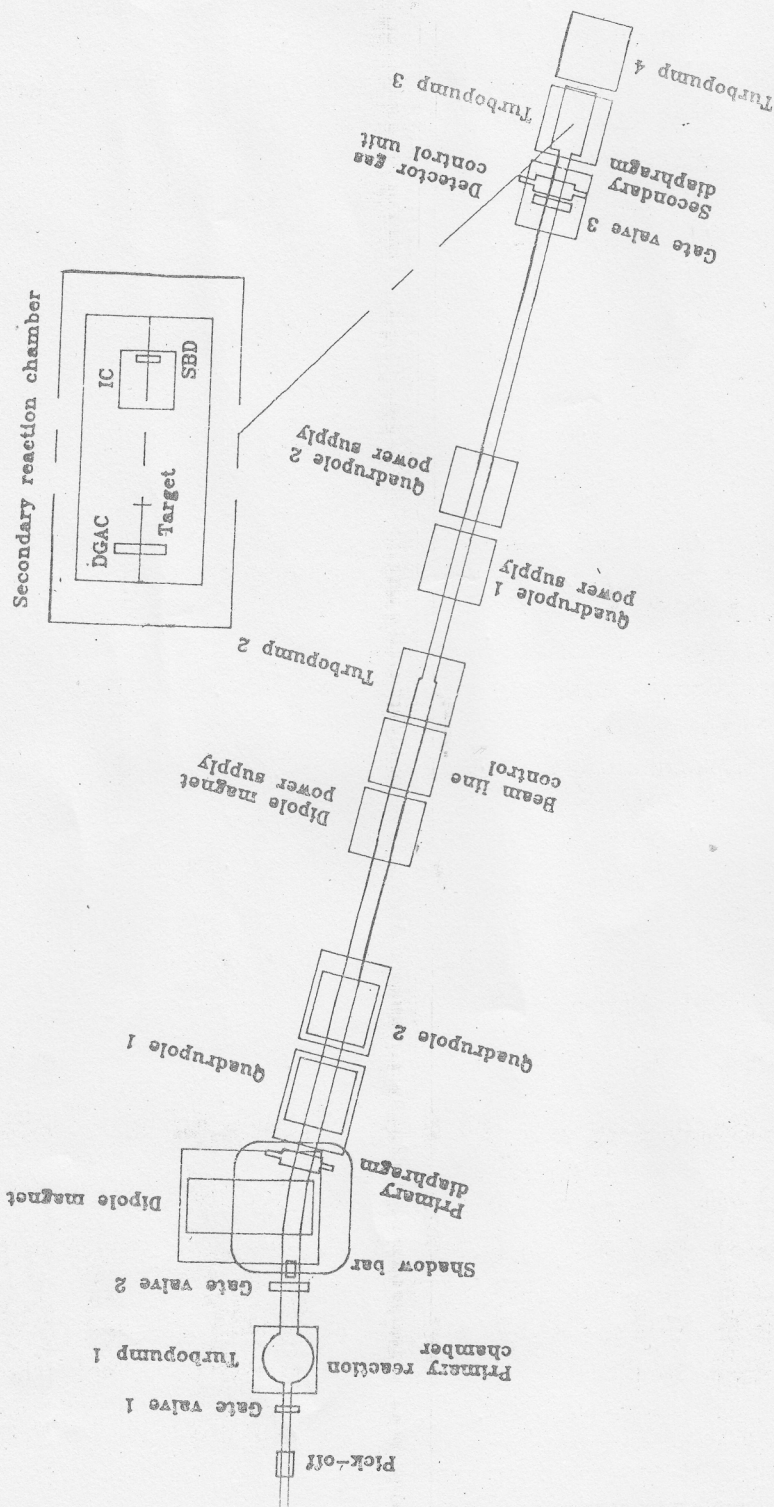


Fig. 1. The experimental arrangement.

3 EXPERIMENTAL ARRANGEMENT

The experimental arrangement is schematically shown in Fig. 1. A gas cell is installed in the primary reaction chamber as the production target. The window of the gas cell is made of 2–3 mg / cm² Mo, Ni or Ti. It can bear a pressure difference up to 162 kPa. The vacuum of the primary reaction chamber is kept at 3×10^{-4} Pa. The dipole and quadrupoles are the decommissioned components of the 1.2 m cyclotron of CIAE. The specifications of these electro-magnetic components are listed in table 1.

Table 1. The specifications of the electro-magnetic components of the secondary beam line

Dipole (D)	Quadrupoles (Q1,Q2)
Magnet gap 10.0 cm	Aperture 13.86 cm
Maximum field 0.65 T	Maximum field gradient 4.35×10^{-2} T / cm
Radius of effective deflection 2.2 m	Effective length 0.36 m
Deflection angle 13°	

A shadow bar was installed between the gas cell and the dipole during the tuning. The sectional view of the acceptable beams near the shadow bar is shown in Fig. 2. As can be seen, 52 % of the primary beam is blocked by the shadow bar, while only 9% of the secondary beam is lost, thus the ¹¹C beam purity has been enhanced from 6 % to 14 %.

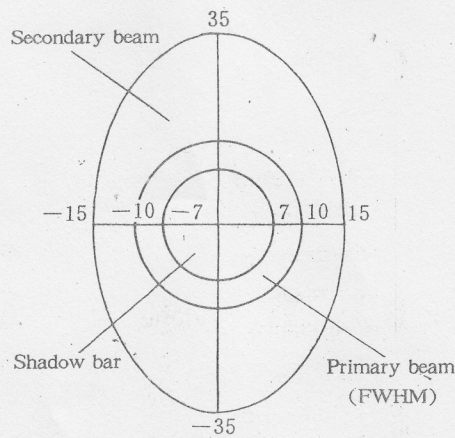


Fig. 2. The sectional view of the acceptable beams near the shadow bar (in mm).

There are a primary diaphragm S1, secondary diaphragm S2 (both with 50 mm dynamic range), and a Φ14 mm aperture along the beam line. The performance of the secondary beam line is listed in Table 2.

Table 2. The performance of the secondary beam line

Maximum solid angle	$\Delta\Omega = 1.8 \text{ msr}$	$(\Delta\theta = \pm 16.4 \text{ mrad}$	$\Delta\varphi = \pm 34.8 \text{ mrad})$
Maximum magnetic rigidity	$B^o = 1.4 \text{ Tm}$		
Total length	$L = 9.8 \text{ m}$		
Dispersion at the focal plane	$\Delta X(\Delta P / P) = 0.47 \text{ cm} / \%$		
Spot size of the secondary beam	$\Delta X = \pm 0.54 \text{ cm}$		$\Delta Y = \pm 0.92 \text{ cm}$
Acceptance angle	0°		
Deflection angle of the beam	13°		

In order to test the secondary beam line and to tune the secondary radioactive beams, we installed in the secondary reaction chamber a double-grid avalanche counter (DGAC) for X / Y position and time information of the beams, an ionization chamber (IC) as the ΔE detector for particle identification and a $\Phi 20 \text{ mm}$ surface barrier detector (SBD) to measure the residual energy E_r . The timing signal from the pick-off or the RF of the tandem accelerator and that of the DGAC were utilized for time of flight measurements.

The required and the measured detector resolutions are listed in Table 3.

Table 3. The time and energy resolutions of the detectors *

	Timing device	Ionization chamber	Surface barrier detector
Required	2.5%	6%	2%
Measured	2%	4.5%	1.0%

* For 60 MeV ^{11}B ions.

4 ^{11}C AND ^{17}F BEAM TUNING

The ^{11}C and ^{17}F beams have been successfully tuned in the experiment. The tuning procedure is as follows:

- check the beam optics calculation using the primary beam;
- set up the magnetic field according to the beam optics calculation for the desired secondary beam and the correction factors obtained from step a;
- identify the pattern corresponding to the ions of the secondary beam in the $\Delta E - E_r$ and / or ΔE -TOF two-dimensional plots;
- pump the gas out from the gas cell, the pattern assigned to the secondary beam should disappear if the identification of the secondary beam is correct;
- optimize the field of the dipole magnet to increase the intensity ratio of the secondary beam to the primary beam contaminants;
- optimize the quadrupole magnetic field to increase the intensity ratio further and to minimize the spot size of secondary beam;
- adjust the diaphragms S1 and S2 to improve the intensity ratio, while not to lose the second-

secondary beam intensity significantly. The calculated and optimized magnetic fields of the dipole and quadrupoles for the ^{11}C and ^{17}F beams are listed in Table 4.

Table 4. The magnetic fields of the dipole and quadrupoles for ^{11}C and ^{17}F beams

Secondary beam	Calculated			Optimized		
	D / T	Q_1 / (T / cm)	Q_2 / (T / cm)	D / T	Q_1 / (T / cm)	Q_2 / (T / cm)
$^{11}\text{C}^{6+}$ 40.6 MeV	0.2392	0.02288	0.01911	0.23604	0.02285	0.01929
$^{17}\text{F}^{9+}$ 67.8 MeV	0.2562	0.02451	0.02047	0.25263	—	—

It is observed that the separation of the secondary beam from the primary beam contaminants strongly depends on the position deviation of the primary beam spot. The influence of the deviation on the ratio of the secondary to primary beams is listed in Table 5.

Table 5. The influence of the position deviation of the primary beam spot on the ratio of ^{11}C to ^{11}B beams*

Ratio	$X=2$ mm	$X=0$ mm	$X=-2$ mm
$Y=2$ mm	—	1.0%	—
$Y=0$ mm	0.2%	3.3%	0.4%
$Y=-2$ mm	—	0.2%	—

* Before optimization and without shadow bar.

Figures 3–5 show the ΔE -Er, TOF- ΔE and Er spectra obtained in the ^{11}C tuning experiment. The horizontal profile of the ^{11}C beam is given in Fig. 6. It can be seen that the ^{11}C beam has been focused into 8 mm (FWHM).

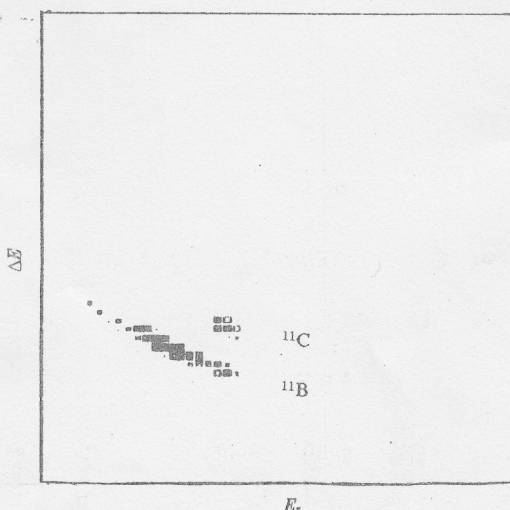


Fig. 3. The ΔE -Er spectrum for ^{11}C .

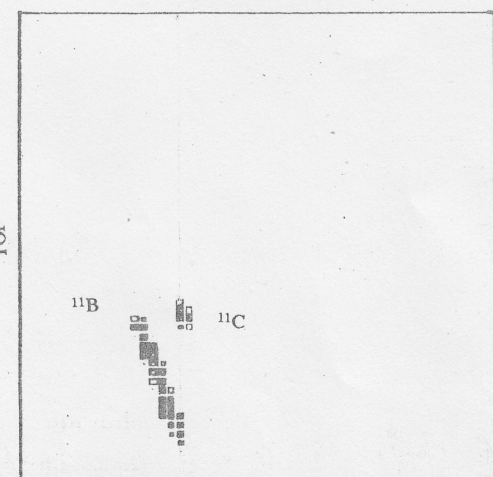


Fig. 4. The TOF- ΔE spectrum for ^{11}C .

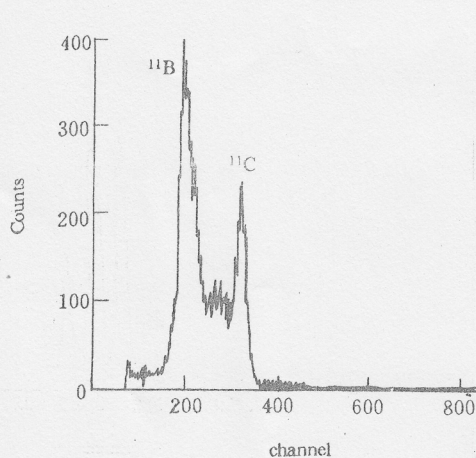


Fig. 5. The E_r spectrum for ^{11}C .

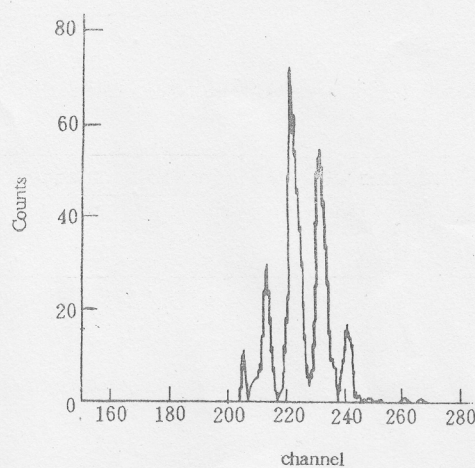


Fig. 6. The horizontal profile of the ^{11}C beam.
The interpeak distance is 2 mm.

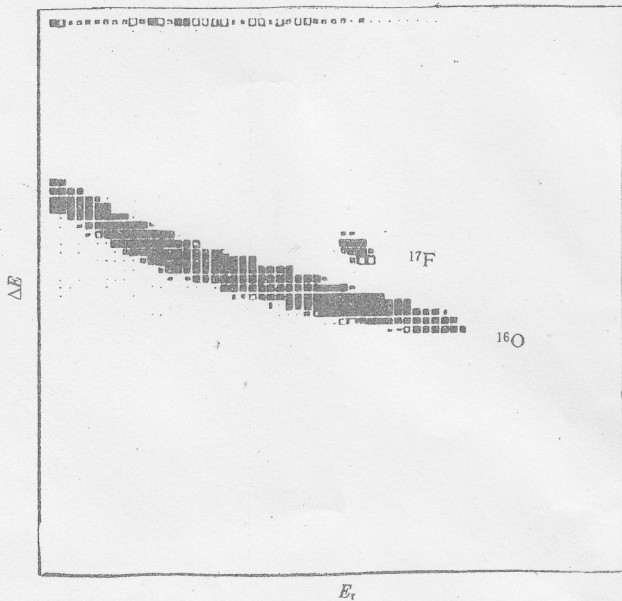


Fig. 7. The $\Delta E - E_r$ spectrum for ^{17}F .

5 COULOMB SCATTERING EXPERIMENT OF ^{11}C BEAM

In order to measure the secondary beam intensity at present conditions a Coulomb scattering experiment of the ^{11}C beam on an Au target was performed. The results are summarized in Table 6. The deduced ^{11}C beam intensity in this experiment is 1.2×10^5 particles / s at ^{11}B beam intensity of 175 enA with the well-known Coulomb scattering cross section.

Table 6. The results of the Coulomb scattering measurement of ^{11}C on Au *

Laboratory Angle / (°)	15	7.5
^{11}B beam average intensity / enA	175	12
Counts per min. for scattered ^{11}C	6.7	7.6
Coulomb scattering cross section / (mb / Sr)	2.76×10^5	4.38×10^6
^{11}C secondary beam intensity / (particles / s)	1.2×10^5	8.5×10^3
Conversion Ratio ($^{11}\text{C} / ^{11}\text{B}$)	5.4×10^{-7}	5.9×10^{-7}

* The solid angle of the detector is 5.8 msr.

6 SUMMARY

The ^{11}C and ^{17}F secondary beams have been successfully delivered with the CIAE secondary beam line. The characteristics of the beams obtained from the experiment are listed in Table 7.

Table 8 gives the comparison of the present ^{11}C secondary beams with the secondary beams obtained at University of Notre Dame ⁽⁴⁾.

Table 7. The characteristics of the ^{11}C and ^{17}F beams obtained in the experiment

Secondary beam	^{11}C	^{17}F
Production reaction	$^1\text{H}(^{11}\text{B}, ^{11}\text{C})\text{n}$	$^2\text{H}(^{16}\text{O}, ^{17}\text{F})\text{n}$
Primary beam	$^{11}\text{B}^{5+}$ 66.12 MeV	$^{16}\text{O}^{7+}$ 88.12 MeV
Secondary beam	$^{11}\text{C}^{6+}$ 41 MeV	$^{17}\text{F}^{9+}$ 68 MeV
Secondary beam energy resolution	1.0 MeV	1.5 MeV
Purity of secondary beam	14 %	0.5 % ⁺
Spot diameter of secondary beam	8 mm	8 mm
Conversion ratio from primary to secondary	5×10^{-7}	1×10^{-6}
Attainable secondary beam intensity *	6×10^6	1.2×10^7

+ Can be larger by using shadow bar.

* Primary beam intensity 1.0 pμA and gas cell pressure 162 kPa.

Table 8. The comparison of the ^{11}C secondary beams

Laboratory	University of Notre Dame, USA	CIAE, P. R. China
Secondary beam	^8Li	^{11}C
Production reaction	$^9\text{Be}(^7\text{Li}, ^8\text{Li})^8\text{Be}$	$^1\text{H}(^{10}\text{B}, ^7\text{Be})^4\text{He}$
Energy / MeV	14.3	22.4
Energy resolution / MeV	0.6	1.0
Spot size / mm	5.0	10.0
Achieved intensity / (particles / s)	$\sim 10^7$	$\sim 10^5$
Conversion ratio	2.2×10^{-7}	4.6×10^{-8}
Angular divergence / (°)	±4	±3

Further amelioration and optimization of the GIRAFFE and nuclear physics experiment with the secondary beams are being undertaken.

REFERENCES

- 1 Myers W D, Nitschke J M, Norman E B. Proc. First Int. Conf. on Radioactive Nuclear Beams. Singapore: World Scientific, 1990.
- 2 Bai Xixiang, Liu Weiping. On the Feasibility of Producing Secondary Radioactive Nuclear Beams Using Reactions in Reversed Geometries at Tandem Accelerator. At Energy Sci Technol, 1993, 27(5): 1.
- 3 Liu Weiping, Li Zhichang, Guan Xialing, et al. Design of a Beam Line for Secondary Radioactive Ions. At Energy Sci Technol, 1993, 27(5): 7.
- 4 Bechetti F D, Liu W Z, Roberts D A, et al.. Measurements of Discrete Nuclear Reactions Induced by a Radioactive ^8Li Beam. Phys Rev, 1989, C40: R1104.